Journal of Sound and Vibration (2000) **237**(4), 697–708
doi:10.1006/jsvi.2000.3043, available online at http://www.idealibrary.com on IDEAL®

FREE VIBRATION ANALYSIS OF ISOSCELES TRIANGULAR MINDLIN PLATES BY THE TRIANGULAR DIFFERENTIAL QUADRATURE METHOD

H. Z. Zhong

Department of Civil Engineering, Tsinghua University, Beijing 100084, *People's Republic of China*

(*Received* 11 *October* 1999, *and in final form* 18 *April* 2000)

The triangular differential quadrature method is applied to the free flexural vibration of isosceles triangular Mindlin plates. The first six frequencies are sought and the convergence of triangular differential quadrature method in vibrational analysis of triangular Mindlin plates is examined. In comparison with available results, good to excellent agreement is achieved for triangular plates with combinations of clamped and simply supported boundary conditions. The implementation of various other boundary conditions in triangular differential quadrature analysis is also discussed and the sensitivity of solution to the implementation of corner conditions in vibrational analysis is highlighted.

1. INTRODUCTION

Vibration of plates has attracted concerns over many years. In comparison with rectangular plates which have been studied intensively [1, 2], triangular plates have received relatively less attention. In addition to the geometric variety of triangles, the combination of boundary conditions is also a challenge. Most efforts devoted to the vibration of triangular plates are in the confines of Kirchhoff plates [3–7]. For thick or moderately thick plates, Mindlin theory [8] has been widely used to take into account the transverse shear effects. In a comprehensive review of vibrational analysis of thick plates, Liew *et al.* [9] pointed out that the publications available for thick and moderately thick triangular plates had been very limited. Using the Rayleigh–Ritz method, Kitipornchai *et al.* [10] studied isosceles triangular Mindlin plates with various apex angles, thickness-to-width ratios and various combinations of boundary conditions. Liew [11] applied the same method to the free vibration of triangular plates with curves internal supports. The vibration of triangular plates subject to isotropic in-plane stresses was also studied by Xiang *et al.* [12]. Other relevant researches on vibration of Mindlin plates with various boundary conditions can be found in the newly published book of Liew *et al.* [13].

The differential quadrature method has been applied widely to various structural problems, especially over the past decade. It stands out as a competitive numerical tool due to its mathematical simplicity and high efficiency and accuracy. However, the conventional differential quadrature method is restricted to problems with domains of regular geometry. For problems with irregular geometric domains, transformation is needed to map an irregular physical domain into a regular computational domain [14–16]. Although the conventional differential quadrature method can be applied to problems with triangular domain, singularity arises which has to be eliminated in the implementation of differential quadrature [17]. As a new numerical method proposed by the author, the triangular

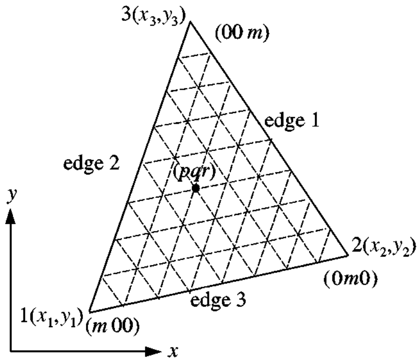

Figure 1. Grid in triangular differential quadrature.

differential quadrature method (TDQM) [18] overcomes the problem of singularity and renders the transformation unnecessary. It has been shown that the triangular differential quadrature method is a very effective and efficient tool in elastostatic analysis of triangular thick plate [19]. In this paper, an attempt is made to study free vibration of some isosceles triangle Mindlin plates using the new numerical method. It is found that for triangular Mindlin plates with various combinations of simply supported boundary condition and fully clamped boundary condition, convergent results for the first six frequencies can be obtained. In comparison with the available data, good to excellent agreement is attained, indicating that the TDQM is an effective numerical tool. In the meantime, the implementation of other boundary conditions in triangular differential quadrature analysis is addressed and the influence of corner condition on solution is discussed.

2. TRIANGULAR DIFFERENTIAL QUADRATURE METHOD

First of all, a triangular domain is first discretized into a uniform grid system. The present exposition of the grid system follows closely the description in reference [18]. The three edges are identified by the opposite vertices, respectively, e.g., edge 1 opposite vertex 1. The normal to an edge identifies the corresponding direction. Parallel lines are drawn which divide the distance between vertex 1 and edge 1 into m equal segments in direction 1. Each line is identified with a digit from 0 to m, the line 0 being coincident with edge 1 and line m passing through vertex 1. A typically line is denoted by p in direction 1. From the intersections of the lines with the other two edges, parallel lines can be drawn with respect to edge 3 and edge 2 respectively. Thus, the grid system is generated (see Figure 1). There are

$$M = (m + 1)(m + 2)/2 \tag{1}$$

grid points in the entire triangular domain. In a similar way, the typical lines in direction 2 (normal to edge 2) and direction 3 (normal to edge 3) are designated as q and r respectively. Apparently, a typical point in the grid system is identified by three digits p, q, r, consistent with the designation of typical lines in the three directions. The area co-ordinates for the typical point are p/m, q/m, r/m. It is evident that

$$p + q + r = m, \quad 0 \leqslant p, q, r \leqslant m. \tag{2}$$

In the triangular differential quadrature method, the partial derivative of a function $f(x, y)$ with respect to a space variable at a given discrete grid point is approximated by a weighted linear summation of the function values at all discrete grid points in the entire triangular domain. Therefore, the approximation of a derivative at a grid point (α, β, γ) is given as

$$D_n\{f(x,y)\}_{\alpha\beta\gamma} = \sum_{j=0}^{m} \sum_{j=0}^{m-j} C^{(n)}_{\alpha\beta\gamma,\,pqr} f_{pqr}, \tag{3}$$

where D_n is a differential operator of order n. The subscript indices (p, q, r) take the following values in the two summation loops:

$$(p,q,r) = (m-i-j, i, j). \tag{4}$$

$C^{(n)}_{\alpha\beta\gamma,\,pqr}$ are the weighting coefficients related to the function values f_{pqr} at points (p, q, r). In his just submitted work, Zhong [19] enunciated two approaches to determine the weighting coefficients. One is an implicit approach in which equation (3) is required to be exact for the following trial functions:

$$f = L_1^p L_2^p L_3^r, \quad 0 \leqslant p, q, r \leqslant m, \tag{5}$$

where the expressions of the three area co-ordinates of an arbitrary point (x, y) inside a triangular domain can be given as

$$L_i = \frac{1}{2\Delta}(a_i + b_i x + c_i y), \quad i = 1, 2, 3. \tag{6}$$

Δ is the area of the triangle which is expressed in terms of the Cartesian co-ordinates of the three vertices as

$$2\Delta = \begin{vmatrix} 1 & x_1 & y_1 \\ 1 & x_2 & y_2 \\ 1 & x_3 & y_3 \end{vmatrix}. \tag{7}$$

The coefficients in equation (6) are the values of the determinants of the corresponding cofactor matrices, e.g.,

$$a_1 = x_2 y_3 - x_3 y_2, \quad b_1 = y_2 - y_3, \quad c_1 = -(x_2 - x_3). \tag{8}$$

The remaining coefficients in equation (6) can be obtained by interchanging the subscripts 1, 2, 3. It is noteworthy that the three vertices should be numbered in an anti-clockwise sequence in order to ensure positive value of the triangular area in equation (7). Apparently, one needs to solve simultaneous algebraic equations to determine $C^{(n)}_{\alpha\beta\gamma,\,pqr}$ in the approach. The alternative is an approach in which explicit formulae are given for the weighting coefficients. In this paper, the explicit formulae are taken, since it is more convenient and straightforward. In this approach, it is required that equation (3) be exact for the following M trial functions

$$f_{pqr} = \bar{f}_p(L_1)\bar{f}_q(L_2)\bar{f}_r(L_3), \quad 0 \leqslant p, q, r \leqslant m, \tag{9}$$

where the auxiliary function is given as

$$\bar{f}_p(L_1) = \begin{cases} \displaystyle\prod_{k=1}^{p} \frac{mL_1 - k + 1}{k}, & 1 \leqslant p \leqslant m, \\ 1 & p = 0. \end{cases} \tag{10}$$

Similar expressions for $\bar{f}_q(L_2)$ and $\bar{f}_r(L_3)$ can be defined. Thus, explicit formulae for the weighting coefficients of the first order derivative are obtained as

$$C^{(x)}_{\alpha\beta\gamma,\,pqr} = \begin{bmatrix} \dfrac{\partial L_1}{\partial x} & \dfrac{\partial L_2}{\partial x} & \dfrac{\partial L_3}{\partial x} \end{bmatrix} \begin{Bmatrix} \dfrac{\partial f_{pqr}}{\partial L_1} \\ \dfrac{\partial f_{pqr}}{\partial L_2} \\ \dfrac{\partial f_{pqr}}{\partial L_3} \end{Bmatrix}_{\alpha\beta\gamma} = \begin{bmatrix} \dfrac{b_1}{2\Delta} & \dfrac{b_2}{2\Delta} & \dfrac{b_3}{2\Delta} \end{bmatrix} \begin{Bmatrix} \dfrac{d\bar{f}_p}{dL_1}\bar{f}_q\bar{f}_r \\ \bar{f}_p\dfrac{d\bar{f}_q}{dL_2}\bar{f}_r \\ \bar{f}_p\bar{f}_q\dfrac{d\bar{f}_r}{dL_3} \end{Bmatrix}_{\alpha\beta\gamma}. \tag{11}$$

Similar expression for $C^{(x)}_{\alpha\beta\gamma,\,pqr}$ can be established, i.e.,

$$C^{(y)}_{\alpha\beta\gamma,\,pqr} = \begin{bmatrix} \dfrac{\partial L_1}{\partial y} & \dfrac{\partial L_2}{\partial y} & \dfrac{\partial L_3}{\partial y} \end{bmatrix} \begin{Bmatrix} \dfrac{\partial f_{pqr}}{\partial L_1} \\ \dfrac{\partial f_{pqr}}{\partial L_2} \\ \dfrac{\partial f_{pqr}}{\partial L_3} \end{Bmatrix}_{\alpha\beta\gamma} = \begin{bmatrix} \dfrac{c_1}{2\Delta} & \dfrac{c_2}{2\Delta} & \dfrac{c_3}{2\Delta} \end{bmatrix} \begin{Bmatrix} \dfrac{d\bar{f}_p}{dL_1}\bar{f}_q\bar{f}_r \\ \bar{f}_p\dfrac{d\bar{f}_q}{dL_2}\bar{f}_r \\ \bar{f}_p\bar{f}_q\dfrac{d\bar{f}_r}{dL_3} \end{Bmatrix}_{\alpha\beta\gamma}. \tag{12}$$

From equation (10), the first order derivative of $\bar{f}_p(L_1)$ with respect to L_1 is obtained as

$$\left.\frac{d\bar{f}_p}{dL_1}\right|_{L_1=\alpha/m} = \begin{cases} m\displaystyle\sum_{k=1}^{p}\frac{\bar{f}_p(\alpha/m)}{\alpha-k+1}, & 2\leqslant p\leqslant\alpha, \\ \dfrac{m}{p!}\displaystyle\prod_{\substack{k=1\\k\neq\alpha+1}}^{p}(\alpha-k+1), & 0\leqslant\alpha\leqslant p-1, \\ m, & p=1, \\ 0, & p=0 \end{cases} \tag{13}$$

Similar expression for the derivatives of $\bar{f}_q(L_2)$ and $\bar{f}_r(L_3)$ with respect to L_2 and L_3 can be derived.

The weighting coefficients for higher order derivatives are obtained through recurrence relationship such as

$$C^{(xx)}_{\alpha\beta\gamma,\,pqr} = \sum_{j=0}^{m}\sum_{j=0}^{m-j} C^{(x)}_{\alpha\beta\gamma,\,stu}C^{(x)}_{stu,\,pqr}, \tag{14a}$$

$$C^{(xy)}_{\alpha\beta\gamma,\,pqr} = \sum_{j=0}^{m}\sum_{j=0}^{m-j} C^{(x)}_{\alpha\beta\gamma,\,stu}C^{(y)}_{stu,\,pqr}, \tag{14b}$$

$$C^{(yy)}_{\alpha\beta\gamma,\,pqr} = \sum_{j=0}^{m}\sum_{j=0}^{m-j} C^{(y)}_{\alpha\beta\gamma,\,stu}C^{(y)}_{stu,\,pqr}. \tag{14c}$$

Analogous to the DQM, the governing differential equation of a physical problem is expressed in terms of the triangular differential quadrature format at interior grid points of the domain. Meanwhile, the boundary conditions at the edges of the domain must be invoked. Equation (3) need be implemented if Neumann-type boundary conditions appear.

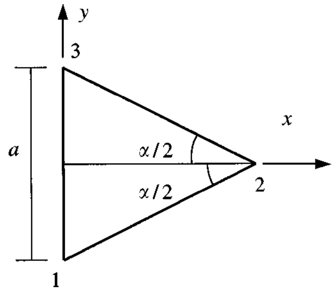

Figure 2. Co-ordinate system of isosceles triangular Mindlin plate.

For mth order triangular differential analysis of Mindlin plates, there are $(m-2)(m-1)/2$ inner grid points at which governing equations are implemented. At the remaining $3m$ boundary discrete points, boundary conditions are prescribed.

3. FORMULATION OF MINDLIN PLATES

3.1. GOVERNING EQUATIONS

In order to make comparison with the available results in reference [10], the same Cartesian co-ordinate system and the orientation of an isosceles triangle are chosen (see Figure 2). In addition, the commonly used non-dimensional frequency parameter is also introduced, i.e.,

$$\lambda = \frac{\omega a^2}{2\pi}(\rho h/D)^{1/2}, \tag{15}$$

where ω is the angular frequency, ρ the mass of the plate per unit area and the flexural rigidity

$$D = \frac{Eh^3}{12(1-\nu^2)}, \tag{16}$$

in which E and ν are Young's modulus and Poisson's ratio respectively.

The governing equations for a homogeneous and isotropic Mindlin plate, in terms of the three displacement components, are given as follows:

$$\beta_1\left(\frac{\partial^2\psi_x}{\partial x^2}+\frac{1-\nu}{2}\frac{\partial^2\psi_x}{\partial y^2}+\frac{1+\nu}{2}\frac{\partial^2\psi_y}{\partial x\partial y}\right)+\beta_2\left(\frac{\partial w}{\partial x}-\psi_x\right)+\lambda^2\psi_x=0, \tag{17a}$$

$$\beta_1\left(\frac{\partial^2\psi_y}{\partial y^2}+\frac{1-\nu}{2}\frac{\partial^2\psi_y}{\partial x^2}+\frac{1+\nu}{2}\frac{\partial^2\psi_x}{\partial x\partial y}\right)+\beta_2\left(\frac{\partial w}{\partial y}-\psi_y\right)+\lambda^2\psi_y=0, \tag{17b}$$

$$\beta_3\left(\frac{\partial^2 w}{\partial x^2}+\frac{\partial^2 w}{\partial y^2}-\frac{\partial\psi_x}{\partial x}-\frac{\partial\psi_y}{\partial y}\right)+\lambda^2 w=0, \tag{17c}$$

where w is the deflection, ψ_x and ψ_y are the rotations of the normal against the two co-ordinate axes y and x respectively; the three constant coefficients are

$$\beta_1=\frac{3a^4}{\pi^2h^2},\quad \beta_2=\frac{18(1-\nu)\kappa a^4}{\pi^2h^4},\quad \beta_3=\frac{3(1-\nu)\kappa a^4}{2\pi^2h^2}, \tag{18}$$

where h, v, κ are the plate thickness, Poisson's ratio and shear correction factor which is calculated based on the Nanni formula [20]

$$\kappa = \frac{20(1+v)}{24+25v+v^2} \tag{19}$$

Introducing the triangular differential quadrature, equation (17) will be recast into a set of algebraic equations at any grid point (α, β, γ), i.e.,

$$\sum_{j=0}^{m}\sum_{j=0}^{m-j}\left[\beta_1\left(C^{(xx)}_{\alpha\beta\gamma,\,pqr}+\frac{1-v}{2}C^{(yy)}_{\alpha\beta\gamma,\,pqr}\right)(\psi_x)_{pqr}+\beta_1\frac{1+v}{2}C^{(xy)}_{\alpha\beta\gamma,\,pqr}(\psi_y)_{pqr}\right.$$
$$\left.+\beta_2 C^{(x)}_{\alpha\beta\gamma,\,pqr}w_{pqr}\right]+(\lambda^2-\beta_2)(\psi_x)_{\alpha\beta\gamma}=0, \tag{20a}$$

$$\sum_{j=0}^{m}\sum_{j=0}^{m-j}\left[\beta_1\left(C^{(yy)}_{\alpha\beta\gamma,\,pqr}+\frac{1-v}{2}C^{(xx)}_{\alpha\beta\gamma,\,pqr}\right)(\psi_y)_{pqr}+\beta_1\frac{1+v}{2}C^{(xy)}_{\alpha\beta\gamma,\,pqr}(\psi_x)_{pqr}\right.$$
$$\left.+\beta_2 C^{(y)}_{\alpha\beta\gamma,\,pqr}w_{pqr}\right]+(\lambda^2-\beta_2)(\psi_y)_{\alpha\beta\gamma}=0, \tag{20b}$$

$$\beta_3\sum_{j=0}^{m}\sum_{j=0}^{m-j}[(C^{(xx)}_{\alpha\beta\gamma,\,pqr}+C^{(yy)}_{\alpha\beta\gamma,\,pqr})w_{pqr}-C^{(x)}_{\alpha\beta\gamma,\,pqr}(\psi_x)_{pqr}-C^{(y)}_{\alpha\beta\gamma,\,pqr}(\psi_y)_{pqr}]$$
$$+\lambda^2 w_{\alpha\beta\gamma}=0, \tag{20c}$$

3.2. BOUNDARY CONDITIONS

There are usually three typical boundary conditions for Mindlin plates. They are:

(a) Clamped edge (C) which can be described symbolically as

$$\psi_x=\psi_y=w=0. \tag{21}$$

(b) Free edge (F) which requires

$$Q_n=M_n=M_{nx}=0, \tag{22}$$

where Q_n, M_n, M_{nx} are the shearing force, bending moment and twisting moment at the edge respectively. Their expressions in terms of the displacements are given as

$$Q_n=\kappa Gh\left[\left(\frac{\partial w}{\partial x}-\psi_x\right)\cos\theta+\left(\frac{\partial w}{\partial y}-\psi_y\right)\sin\theta\right], \tag{23a}$$

$$M_n=-D\left(\frac{\partial\psi_x}{\partial x}+v\frac{\partial\psi_y}{\partial y}\right)\cos^2\theta-(1-v)D\left(\frac{\partial\psi_x}{\partial y}+\frac{\partial\psi_y}{\partial x}\right)\cos\theta\sin\theta$$
$$-D\left(\frac{\partial\psi_y}{\partial y}+v\frac{\partial\psi_x}{\partial x}\right)\sin^2\theta, \tag{23b}$$

$$M_{ns}=-D(1-v)\left(\frac{\partial\psi_y}{\partial y}-\frac{\partial\psi_x}{\partial x}\right)\cos\theta\sin\theta-\frac{D(1-v)}{2}\left(\frac{\partial\psi_x}{\partial y}+\frac{\partial\psi_x}{\partial x}\right)(\cos^2\theta-\sin^2\theta), \tag{23c}$$

where G is the shear modulus and θ the angle formed by the outward normal of the edge with the x-axis.

(c) Simply-supported edge. There are two types of simply supported edges in Mindlin plate theory. The first type (S) requires

$$w = 0, \quad M_n = 0, \quad \psi_x = -\psi_x \sin\theta + \psi_y \cos\theta = 0. \tag{24}$$

The second type (S*) is described mathematically as

$$w = 0, \quad M_n = 0, \quad M_{ns} = 0. \tag{25}$$

The assembly of the triangular differential quadrature analog of equations (20) at all inner grid points and the boundary condition equations at the three edges of the triangle results in a set of $3M$ algebraic equations which can be written in matrix form as

$$\begin{bmatrix} [K_{bb}] & [K_{bi}] \\ [K_{ib}] & [K_{ii}] \end{bmatrix} \begin{Bmatrix} \{\Theta_b\} \\ \{\Theta_i\} \end{Bmatrix} = \begin{Bmatrix} \{0\} \\ \lambda^2 \{\Theta_i\} \end{Bmatrix}, \tag{26}$$

where $\{\Theta_b\}$ is the displacement vector at the three edges of the triangle, and $\{\Theta_i\}$ the displacement vector at all inner grid points. By eliminating the $\{\Theta_b\}$ vector, the above equations become a standard eigenvalue problem of size $[3(m-2)(m-1)/2] \times [3(m-2)(m-1)/2]$, i.e.,

$$[K]\{\Theta_i\} = \lambda^2 \{\Theta_i\}. \tag{27}$$

The eigenvalues of matrix $[K]$ are then extracted using a double QR algorithm [21].

4. RESULTS AND DISCUSSION

In order to simplify the presentation, the isosceles triangles are designated by the abbreviated letters of the boundary condition types at the three edges in left, bottom and top sequence. The objective of the present research is focused on the validation of the triangular differential quadrature method in vibrational analysis since extensive results can be found elsewhere [10]. In this section, presentation of results is centered on the discussion of the implementation of corner conditions in triangular differential quadrature analysis. The basic reason is that the triangular differential quadrature is found to be sensitive to the implementation of corner conditions in vibrational analysis. As an exception, the boundary conditions of CCC triangular plates are consistent around the periphery. Therefore, convergence study is first conducted on CCC isosceles triangular plates with the apex angles $\alpha = 30°, 90°$ and thickness-to-width ratios $h/a = 0{\cdot}001, 0{\cdot}2$. The results are listed in Table 1. It can be seen that good to excellent agreement is achieved in comparison with the results of Kitipornchai *et al.* [10]. In the present TDQ analysis, it is found that the convergence is achieved relatively quickly with the increase of m for thick plates in comparison with that of thin plates. In other words, the results of thick plates are more accurate for a given m than those of thin plates. It is believed that the more flexural deformation of thin plates accounts for the relatively slow convergence. When m is increased to 19, the first six frequencies for both thin plates and thick plates are in good agreement with those of reference [10]. Thus, the grid for $m = 20$ is used as a workhorse throughout all later computations. It should be mentioned that all available results of triangular Mindlin plates with simply supported boundary conditions are based on the second type (S*). Investigation shows, however,

TABLE 1

Convergence of the first six non-dimensional frequencies of CCC plates

α	h/a	m	Mode sequences 1	2	3	4	5	6
30	0·001	15	8·5674	14·0530	17·7861	18·6160	21·1216	26·0337
		16	8·5580	13·7008	18·7772	25·4345	26·4802	32·7133
		17	8·5599	13·5903	18·8974	19·7921	27·4283	29·4766
		18	8·5653	13·6259	18·8696	19·1029	26·7290	28·5508
		19	8·5605	13·6518	18·8272	19·4240	24·5210	27·1600
		20	8·5569	13·6475	18·8289	19·6217	25·7273	26·8060
		[10]	8·5619	13·6434	18·8432	19·5516	26·9655	27·0990
	0·2	15	5·6212	7·9774	10·1326	10·3642	13·4412	13·6826
		16	5·6123	7·9885	10·1203	10·3480	12·5803	13·1394
		17	5·6213	7·9901	10·1185	10·4340	12·5718	13·0332
		18	5·6212	7·9891	10·1205	10·4371	13·0578	13·0645
		19	5·6213	7·9886	10·1210	10·4231	12·9838	13·0905
		20	5·6212	7·9889	10·1207	10·4220	12·8847	13·0884
		[10]	5·6212	7·9888	10·1206	10·4243	12·9099	13·0829
90	0·001	15	29·7969	50·1458	62·5623	95·6297	104·2519	113·3554
		16	29·8817	50·1677	61·8087	76·4852	109·6254	139·5208
		17	29·8170	50·2272	61·9901	76·7771	87·1895	106·7451
		18	29·8707	50·2192	61·9252	77·4088	87·4045	105·8750
		19	29·8337	50·2163	62·0480	77·3041	88·6713	105·7606
		20	29·8601	50·2230	61·9280	77·2480	88·4729	107·2100
		[10]	29·8525	50·2210	62·0064	77·3491	88·5043	107·4329
	0·2	15	12·8976	18·2080	20·9132	24·2840	26·5037	29·9588
		16	12·8951	18·2072	20·9186	24·3152	26·5848	29·9095
		17	12·8972	18·2071	20·9163	24·3055	26·6282	29·9684
		18	12·8953	18·2070	20·9175	24·3019	26·6159	30·0035
		19	12·8969	18·2071	20·9162	24·3030	26·6100	29·9953
		20	12·8955	18·2070	20·9173	24·3031	26·6115	29·9886
		[10]	12·8961	18·2071	20·9168	24·3032	26·6125	29·9922

that the triangular differential quadrature analysis of Mindlin plates under simply supported boundary conditions of the second type (S*) does not converge, even for elastostatic analysis. Therefore, all simply supported edges in TDQ analysis of Mindlin plates are prescribed as the first-type (S). Generally, speaking, there are following six possibilities that a corner may be formed: CC, SC, FC, SS, FS, FF. The two letters represent the boundary condition types of the two edges that form the corner. For the first three cases CC, SC and FC, the boundary conditions for clamped edge—(21) are implemented at the corner. This bears great resemblance to the conventional differential quadrature analysis where Dirichlet boundary conditions are favored against Neumann boundary conditions [17].

For cases SS, FS, FF, the implementation of corner conditions becomes rather thorny. One can only implement partially the boundary conditions at the two edges that form the corner. Take SS as an example. Unlike in elastostatic analysis where the boundary conditions of either edge can be implemented successfully at the corner, it seems that vibrational analysis requires evenhanded treatment of the corner. Assume that θ_1, θ_2 are the directional angles of the two edge normals. The following five conditions coexist at an SS

TABLE 2

*Comparison of the present results of CSS with those of CS*S* [10]*

$\alpha°$	h/a	Mode sequences 1	2	3	4	5	6
30	0·001	5·180 (5·180)	9·325 (9·345)	13·69 (13·66)	14·36 (14·33)	20·20 (20·44)	20·89 (20·86)
	0·2	4·142 (4·045)	6·716 (6·513)	9·001 (8·901)	9·325 (9·062)	11·95 (11·69)	12·26 (12·04)
40	0·001	6·670 (6·650)	13·00 (12·95)	16·23 (16·27)	20·78 (20·79)	26·48 (26·49)	29·42 (29·41)
	0·2	5·039 (4·913)	8·533 (8·275)	10·13 (10·00)	12·08 (11·76)	14·33 (14·05)	15·41 (15·19)
50	0·001	8·343 (8·402)	17·37 (17·36)	19·21 (19·24)	28·78 (28·80)	33·00 (33·02)	34·18 (34·17)
	0·2	6·011 (5·852)	10·48 (10·16)	11·30 (11·16)	14·97 (14·61)	16·45 (16·12)	16·88 (16·75)
60	0·001	10·55 (10·53)	22·71 (22·72)	22·83 (22·83)	37·59 (37·70)	40·68 (40·64)	40·69 (40·68)
	0·2	7·081 (6·883)	12·56 (12·20)	12·58 (12·39)	17·76 (17·45)	18·67 (18·27)	18·68 (18·45)
70	0·001	13·55 (13·18)	26·87 (26·89)	30·57 (29·67)	45·03 (44·64)	49·71 (49·73)	54·25 (52·84)
	0·2	8·279 (8·034)	13·93 (13·73)	14·87 (14·43)	19·66 (19·48)	21·01 (20·52)	21·82 (21·40)
80	0·001	18·21 (16·54)	32·06 (13·02)	40·62 (38·29)	53·88 (52·37)	60·59 (60·45)	72·77 (69·36)
	0·2	9·645 (9·345)	15·48 (15·23)	17·41 (16·90)	21·53 (21·37)	23·48 (22·88)	25·54 (25·04)
90	0·001	20·99 (20·94)	38·54 (38·54)	49·15 (49·16)	62·47 (62·52)	72·98 (73·24)	90·27 (90·22)
	0·2	11·23 (10·87)	17·26 (16·94)	20·19 (19·61)	23·78 (23·62)	26·07 (25·33)	28·18 (26·62)

Note: The data in parentheses are given by Kitipornchai *et al.* [10].

corner:

$$\psi_{s1} = -\psi_x \sin\theta_1 + \psi_y \cos\theta_1 = 0, \quad \psi_{s2} = -\psi_x \sin\theta_2 + \psi_y \cos\theta_2 = 0, \tag{28}$$

$$w = 0, \quad M_{n1} = 0, \quad M_{n2} = 0.$$

One option that achieves success in elastostatic analysis is to consider the first three conditions in equation (28). This is identical to the implementation of clamped edge conditions. It is found that this strategy in vibration analysis works only when m is taken as even numbers for SSS triangular plates. The second option was also attempted in which the last three conditions in equation (28) are implemented. Unfortunately, no convergent results were produced. Nevertheless, under some combinations of boundary conditions, convergent results can still be obtained. In the case of CSS or SCS where there is an SS corner, the results converge satisfactorily when the first three conditions of equation (28) are

TABLE 3

Frequencies λ of triangular plates with CSC boundary conditions

$\alpha°$	h/a	Mode sequences 1	2	3	4	5	6
30	0·001	6·747	11·38	16·15	16·85	23·16	23·80
	0·05	6·554	10·87	15·20	15·79	21·42	21·96
	0·10	6·062	9·718	13·22	13·67	17·89	18·39
	0·15	5·461	8·458	11·23	11·57	14·77	15·17
	0·20	4·874	7·340	9·587	9·847	12·37	12·70
40	0·001	8·457	15·38	19·06	23·82	29·95	33·12
	0·05	8·157	14·49	17·74	21·89	27·06	29·69
	0·10	7·419	12·59	15·13	18·24	22·00	23·89
	0·15	6·567	10·68	12·66	12·66	17·79	19·18
	0·20	5·774	9·098	10·70	12·51	14·70	15·79
50	0·001	10·50	20·28	22·38	32·46	36·97	38·28
	0·05	10·03	18·76	20·58	29·09	32·75	33·78
	0·10	8·957	15·82	17·20	23·32	25·86	26·60
	0·15	7·785	13·10	14·18	18·67	20·52	21·09
	0·20	6·747	10·98	11·85	15·33	16·77	17·22
60	0·001	13·00	26·27	26·30	42·14	45·22	45·28
	0·05	12·27	23·82	23·87	36·75	39·06	39·18
	0·10	10·73	19·47	19·50	28·47	29·94	30·06
	0·15	9·147	15·73	5·84	22·32	23·35	23·46
	0·20	7·816	12·98	13·13	18·12	18·90	18·99
70	0·001	16·07	30·96	33·82	49·86	55·10	58·31
	0·05	14·98	27·63	29·96	42·46	46·36	48·71
	0·10	12·79	22·07	23·64	32·07	34·54	35·97
	0·15	10·69	17·63	18·72	24·82	26·53	26·53
	0·20	9·013	14·45	15·27	19·99	21·28	22·00
80	0·001	20·10	36·76	43·56	58·69	66·71	76·82
	0·05	18·34	32·18	37·28	48·54	54·48	60·89
	0·10	15·25	25·04	28·40	35·74	39·41	43·26
	0·15	12·49	19·69	22·03	27·29	29·83	32·46
	0·20	10·38	15·99	17·77	21·82	23·74	25·69
90	0·001	25·11	44·19	55·29	69·66	80·62	98·29
	0·05	22·59	37·74	46·00	56·17	63·54	75·03
	0·10	18·21	28·54	33·80	40·18	44·66	51·35
	0·15	14·60	22·07	25·74	30·24	33·35	37·89
	0·20	11·98	17·77	20·54	24·00	26·35	29·14

implemented at the SS corner. It is interesting to notice that the present results of CSS are in very good agreement with those of the CS*S* obtained by Kitipornchai [10]. Comparison is made in Table 2.

As a supplementary to the vast available data published in Kitipornchai's work, two combinations of boundary conditions CSC and SCS, which are not included in their work, are studied. The results are presented in Tables 3 and 4. In all computations, it is observed that the frequencies decrease as the increase of plate thickness. For a given plate thickness, the frequencies increase with the apex angle α. It should be mentioned that these phenomena were also reported in Kitipornchai's work [10].

TABLE 4

Frequencies λ of triangular plates with SCS boundary conditions

		Mode sequences					
α°	h/a	1	2	3	4	5	6
30	0·001	6·264	10·60	15·10	15·98	20·96	23·10
	0·05	5·773	9·904	14·13	14·69	20·30	20·68
	0·10	5·418	9·002	12·50	12·92	17·24	17·65
	0·15	4·960	7·967	10·77	11·11	14·41	14·76
	0·20	4·490	7·011	9·290	9·564	12·17	12·47
40	0·001	7·443	13·83	17·51	21·91	27·80	39·23
	0·05	7·002	13·02	16·21	20·18	25·29	27·87
	0·10	6·501	11·58	14·15	17·22	21·04	22·90
	0·15	5·881	10·04	12·06	14·43	17·29	18·66
	0·20	5·268	8·700	10·31	12·20	12·20	15·50
50	0·001	8·865	17·82	20·00	29·43	33·74	35·28
	0·05	8·429	16·70	18·52	26·70	30·35	31·46
	0·10	7·733	14·51	15·94	22·05	24·67	25·45
	0·15	6·908	12·34	13·43	18·04	19·96	20·50
	0·20	6·122	10·54	11·39	15·02	15·02	16·91
60	0·001	10·53	22·73	22·82	37·80	40·58	40·67
	0·05	10·12	21·07	21·20	33·68	36·05	36·10
	0·10	9·164	17·85	17·97	26·98	28·62	28·63
	0·15	8·076	14·89	14·95	21·61	22·80	22·80
	0·20	7·080	12·56	12·58	17·76	18·67	18·68
70	0·001	12·80	26·46	28·94	44·15	48·90	51·88
	0·05	12·18	24·77	26·39	38·79	42·51	44·80
	0·10	10·86	20·22	21·77	30·42	30·42	34·44
	0·15	9·428	16·62	17·80	24·04	25·86	26·94
	0·20	8·175	13·88	14·82	19·59	21·00	21·83
80	0·001	15·64	30·87	36·63	51·13	58·51	67·99
	0·05	14·73	27·99	32·77	44·12	49·678	56·10
	0·10	12·90	22·88	26·27	33·90	37·61	41·65
	0·15	11·02	18·56	21·07	26·47	29·13	31·97
	0·20	9·451	15·37	17·34	21·42	23·47	25·63
90	0·001	19·31	36·46	46·38	59·96	69·81	85·76
	0·05	17·99	32·58	40·44	50·85	57·91	69·31
	0·10	15·42	26·06	31·44	38·17	42·67	49·71
	0·15	12·95	20·84	24·77	29·43	32·62	32·62
	0·20	10·98	17·11	20·16	23·64	26·09	26·93

5. CONCLUDING REMARKS

Attempts have been made to study the free vibration of triangular Mindlin plates using the triangular differential quadrature method. The implementation of corner conditions has been discussed in length. For isosceles triangular plates with CCC, CSS, CSC and SCS boundary conditions, convergent results are obtained. Good to excellent agreement has been achieved in comparison with the available data. For other combinations of boundary conditions, the results were unstatisfactory. It is believed that the uneven performance of TDQ in vibrational analysis is attributed to the sensitivity of implementation of corner condition. Despite the disadvantage, the triangular differential quadrature method still deserves consideration for its mathematical simplicity and straightforward implementation. Since the method is in its infancy, further efforts are clearly needed to enable the TDQ to deal with domains with various corner conditions.

REFERENCES

1. A. Q. LEISSA 1973 *Journal of Sound and Vibration* **31**, 257–293. The free vibration of rectangular plates.
2. D. J. GORMAN 1982 *Free Vibration Analysis of Rectangular Plates*. New York: Elsevier.
3. D. J. GORMAN 1986 *Journal of Sound and Vibration* **106**, 419–413. Free vibration analysis of right triangular plates with combinations of clamped-simply supported boundary conditions.
4. D. J. GORMAN 1989 *American Institute of Aeronautics and Astronautics Journal* **27**, 647–651. Accurate analytical solution for free vibration of the simply supported triangular plate.
5. C. S. KIM and S. M. DICKINSON 1990 *Journal of Sound and Vibration* **141**, 291–311. The free flexural vibration of right triangular isotropic and orthotropic plates.
6. S. MIRZA and M. BIJILANI 1983 *AIAA Journal* **21**, 1472–1475. Vibration of triangular plates.
7. S. MIRZA and M. BIJILANI 1985 *Computers and Structures* **21**, 1129–1135. Vibration of triangular plates of variable thickness.
8. R. D. MINDLIN 1951 *Transactions of the ASME Journal of Applied Mechanics* **18**, 1031–1036. Influence of rotatory inertia and shear in flexural motion of isotropic, elastic plate.
9. K. M. LIEW, Y. XIANG and S. KITIPORNCHAI 1995 *Journal of Sound and Vibration* **180**, 163–176. Research on thick plate vibration: a literature survey.
10. S. KITIPORNCHAI, K. M. LIEW, Y. XIANG and C. M. WANG 1993 *International Journal of Mechanical Science* **35**, 89–102. Free vibration of isosceles triangular Mindlin plates.
11. K. M. LIEW 1993 *Journal of Sound and Vibration* **165**, 329–340. On the use of pb-2 Rayleigh–Ritz method for free-flexural vibration of triangular plates with curved internal supports.
12. Y. XIANG, K. M. LIEW, S. KITIPORNCHAI and C. M. WANG 1994 *Transactions of the ASME Journal of Vibration and Acoustics* **116**, 61–66. Vibration of triangular Mindlin plates subject to isotropic in-plane stresses.
13. K. M. LIEW, C. M. WANG, Y. XIANG and S. KITIPORNCHAI 1998 *Vibration of Mindlin Plates: Programming the p-Version Ritz Method*. Oxford: Elsevier Science.
14. H. Z. ZHONG and Y. H. HE 1998 *International Journal of Solids and Structures* **35**, 2805–2819. Solution of Poisson and Laplace equations by quadrature element method.
15. K. M. LIEW and J. B. HAN 1997 *Communications in Numerical Method in Engineering* **13**, 73–81. A four-node differential quadrature method for straight-sided quadrilateral Reissner/Mindlin plates.
16. J. B. HAN and K. M. LIEW 1997 *Computer Methods in Applied Mechanics and Engineering* **141**, 265–280. An eight-node differential quadrature formulation for curvilinear Mindlin plates.
17. H. Z. ZHONG 1998 *Communications in Numerical Method in Engineering* **14**, 195–208. Elastic Torsional analysis of prismatic shafts by differential quadrature method.
18. H. Z. ZHONG 2000 *Communications in Numerical Method in Engineering*. Triangular differential quadrature (to appear).
19. H. Z. ZHONG 2000 *International Journal of Solids and Structures*. Triangular differential quadrature and its application to elastostatic analysis of Reissner plates (to appear).
20. J. NANNI 1971 *Zeitschriftf angewandte Mathematik und Physik* **22**, 156–185. Das Eulersche Knickproblem unter berucksichtigung der querkrafte.
21. W. H. PRESS, B. P. FLANNERY, S. A. TEUKOLSKY and W. T. VETTERLING 1986 *Numerical Recipes—The Art of Scientific Computing*. Cambridge: Cambridge University Press.